3.3 GROWTH CHARACTERISTICS OF LABORATORY GROWN ICE CRYSTALS BETWEEN -20 °C AND -70 °C.

Matthew P. Bailey* and J. Hallett
Desert Research Institute, Reno Nevada

1. INTRODUCTION

Knowledge of the physical characteristics of ice crystals in glaciated clouds is critical to understanding and modeling the Earth's atmosphere. In situ observations as well as laboratory studies of ice crystals have provided much insight concerning this aspect of the atmosphere though both approaches have limitations.

In situ observations provide brief snapshots of crystal habits in limited regions of clouds, but the sites where the crystals are collected may or may not be well correlated with those in which growth occurred. Microphysical measurements of ice supersaturation, especially at temperatures below approximately -40°C, have also presented difficulties in assessing growth conditions from in situ observations.

Laboratory experiments have provided growth and habit data under controlled conditions of temperature and ice supersaturation but many of these have been skewed by laboratory artifacts and hence are not representative of conditions in the atmosphere. The classical habit diagrams addressing crystal habit as a function of ice supersaturation or excess vapor density have typically yielded results which compare poorly with the real atmosphere for temperatures below -20°C.

In depth analysis of a comprehensive laboratory study of ice crystal growth utilizing a static diffusion chamber has recently been completed. Nucleation, crystal habit, habit distribution and growth rates have been measured as a function of temperature, ice supersaturation and pressure. These characteristics have been measured for temperatures ranging from -20°C to -70°C, supersaturations ranging from 1% with respect to ice to well over water saturation, and pressures commensurate with the standard atmosphere for the temperatures given. Crystals were grown on clean glass filaments approximately 50 :m in diameter. Additionally, fine particles of kaolinite and silver iodide adhering to clean glass filaments were used to measure critical supersaturations for nucleation and the effects of these nucleating agents on crystal habit. A comparison of these results with previous laboratory investigations and in situ observations will be found in Bailey and Hallett (2002a). A summary of these results presented here will show that, contrary to the classical habit diagrams, the crystal habit between -20°C to -40°C is predominantly plate-like and is dominated by polycrystalline forms. Columnar growth occurs predominantly below -40°C and is still dominated by polycrystalline forms as bullet rosettes for sufficiently high ice supersaturation. This aspect of the study demonstrates that the "prism" or columnar description found in habit diagrams below -20°C is largely due to the effects of nucleation method and a misinterpretation of "prism" forms.

Habit distributions and growth rates for temperatures ranging from -20°C to -70°C have been measured in the laboratory and a summary of these is presented. Growth rates include maximum linear dimensional (D) growth rates (dD/dt, diameters in the case of plate-like habits and lengths in the case of columnar forms), maximum projected area growth rates, and volume growth rates. These results can be used to predict the evolution of ice crystal populations in terms of size distribution, radiative characteristics due to crystal area and thickness, and mass growth rate due to volume. They can also be used to infer ice supersaturation and fall velocity/ventilation effects via habit observations. A hypothesis addressing halo crystal growth conditions is also presented.

Corresponding author address: Matthew Bailey, Desert Research Institute, 2215 Raggio Parkway, Reno, Nv 89512; emailL bailey@dri.edu.

2. EXPERIMENTAL METHOD

A schematic of the thermal diffusion chamber used in this study is shown in figure 1 along with an example of temperature and super-

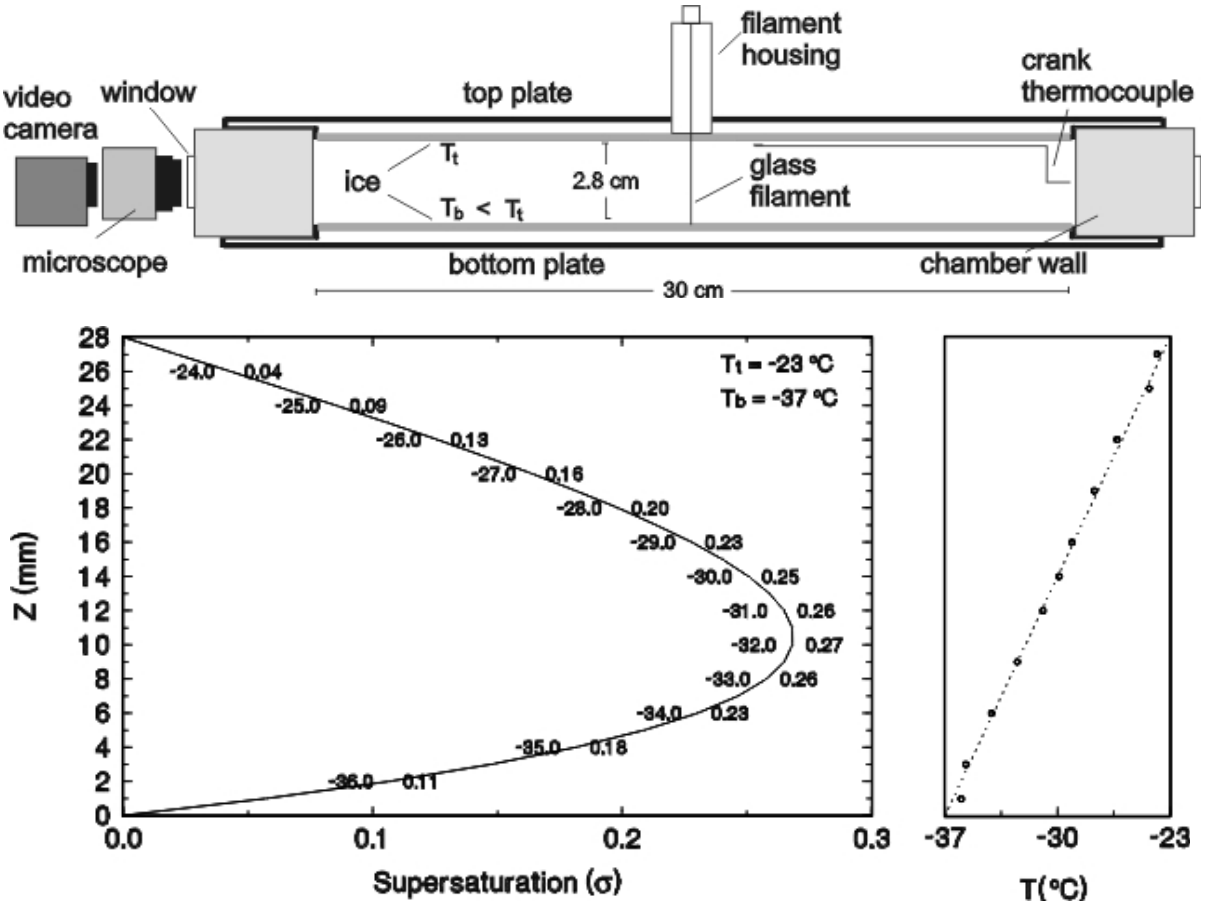

Figure1. Schematic of the static diffusion chamber used in the study. The lower part of the figure is the temperature and supersaturation profile for top and bottom plate temperatures of -23°C and -37°C, respectively, along with the linear temperature profile as measured with a rotatable or crank thermocouple.

saturation profiles for a particular set of top and bottom plate temperatures. The chamber consists of two stainless steel plates separated by a short thick acrylic cylinder which yields an inner chamber diameter of approximately 30 cm and a plate separation of 2.8 cm for a width to height ratio in excess of 10:1. The top and bottom plates are coated with ice and ice supersaturation is determined by the plate temperatures. This large width to height ratio and thick insulation around the entire chamber is necessary to achieve the linear temperature profiles shown. Diffusion chambers with smaller aspect ratios and insufficient insulation are subject to thermal edge effects which creates convection in the chamber, disturbing the expected temperature and supersaturation profiles predicted from the Clausius-Clapeyron relation. Time lapse photography was performed with a video camera and a long working distance Wild microscope.

A linear temperature and vapour density profile between the top and bottom plates together with the exponentially varying equilibrium vapour pressure over ice surfaces in the chamber creates the nonlinear supersaturation as a function of height shown in the figure. In principle, a crystal grown at a particular supersaturation under static conditions is

approximately equivalent to a crystal falling at terminal velocity at a lower supersaturation, the ventilation effect yielding a higher effective supersaturation equivalent to the static value (Keller and Hallett, 1982). Ventilation effects are negligible for small crystals with small fall velocities but increase with increasing crystal size.

3. CRITICAL SUPERSATURATIONS AND NUCLEATION

Critical supersaturations for the nucleation of ice crystals on clean glass filaments and filaments lightly coated with particles of kaolinite or silver iodide are shown in figure 2. Glass and

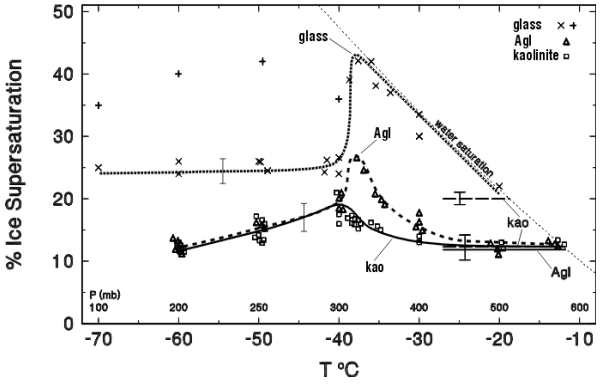

Figure 2. Critical supersaturations for nucleation on clean glass filaments, kaolinite, and silver iodide as a function of temperature and pressure. The + symbols represent ice supersaturations below -40°C where approximately a doubling of the number of nucleated sites on glass filaments occurred.

kaolinites both consist of silicates with mixtures of other compounds and are quite different from silver iodide in terms of crystallographic structure, silver iodide having nearly the same hexagonal crystallographic orientation as ice-I_h. Details of the critical supersaturation measurements can be found in Bailey and Hallett (2002a), however the most important aspect of this study is the abrupt change in nucleability for glass below -40°C and a similar but less pronounced change for kaolinite and silver iodide. Silicates and kaolinites are common materials found in natural ice nuclei and these measurements indicate that ice supersaturations ranging from approximately 12% to 25% with respect to ice are sufficient for heterogenous nucleation below -40°C at reduced pressures.

To nucleate ice crystals in the static diffusion chamber below the critical supersaturation for nucleation on glass (approximately 25% for temperatures below -40°C), a clean glass filament was inserted into the chamber with the top and bottom plate temperatures set to the desired subclinical supersaturation. The chamber was then slowly evacuated to just above the target pressure. A quick reduction in pressure of 5 to 10 mb (hPa) over 1 or 2 seconds affected a quick quasi- adiabatic expansion, raising the supersaturation briefly to the critical value, causing nucleation and followed by growth at the lower preset supersaturation. At or above the critical supersaturation, the glass filament was retained inside the filament housing at a temperature approximately isothermal with the top plate while the chamber was evacuated. After the target pressure was reached, the filament was lowered into the chamber where nucleation was spontaneous. Below water saturation, this method led to the nucleation of well dispersed crystals along the length of the filament so that the particle density along the thread was held to a minimum, eliminating or reducing vapor competition or shadowing effects between neighboring crystals. This was also the case for moderately high ice supersaturations (up to 50%) for temperatures below -40°C where the term "water saturation" is no longer relevant considering the short lifetimes of supercooled pure water droplets below this temperature. For temperatures above -40°C and for ice supersaturations above water saturation, vapor competition was significant, but well separated crystals could still be obtained in many instances and only these crystals were used to obtain growth data under these conditions.

4. HABIT RESULTS

A sample of habit results obtained by the method described are shown in figure 3 which include some linear dimension (D) growth rates for comparison. Pressures approximately equivalent to those of the standard atmosphere for the stated temperatures are displayed near the top of the graph. The crystals shown range in size from 70 μm to approximately 700 μm, though growth rates were calculated from crystals that had grown to sizes between 100 μm and 300 μm, the larger crystal sizes being shown for habit clarity.

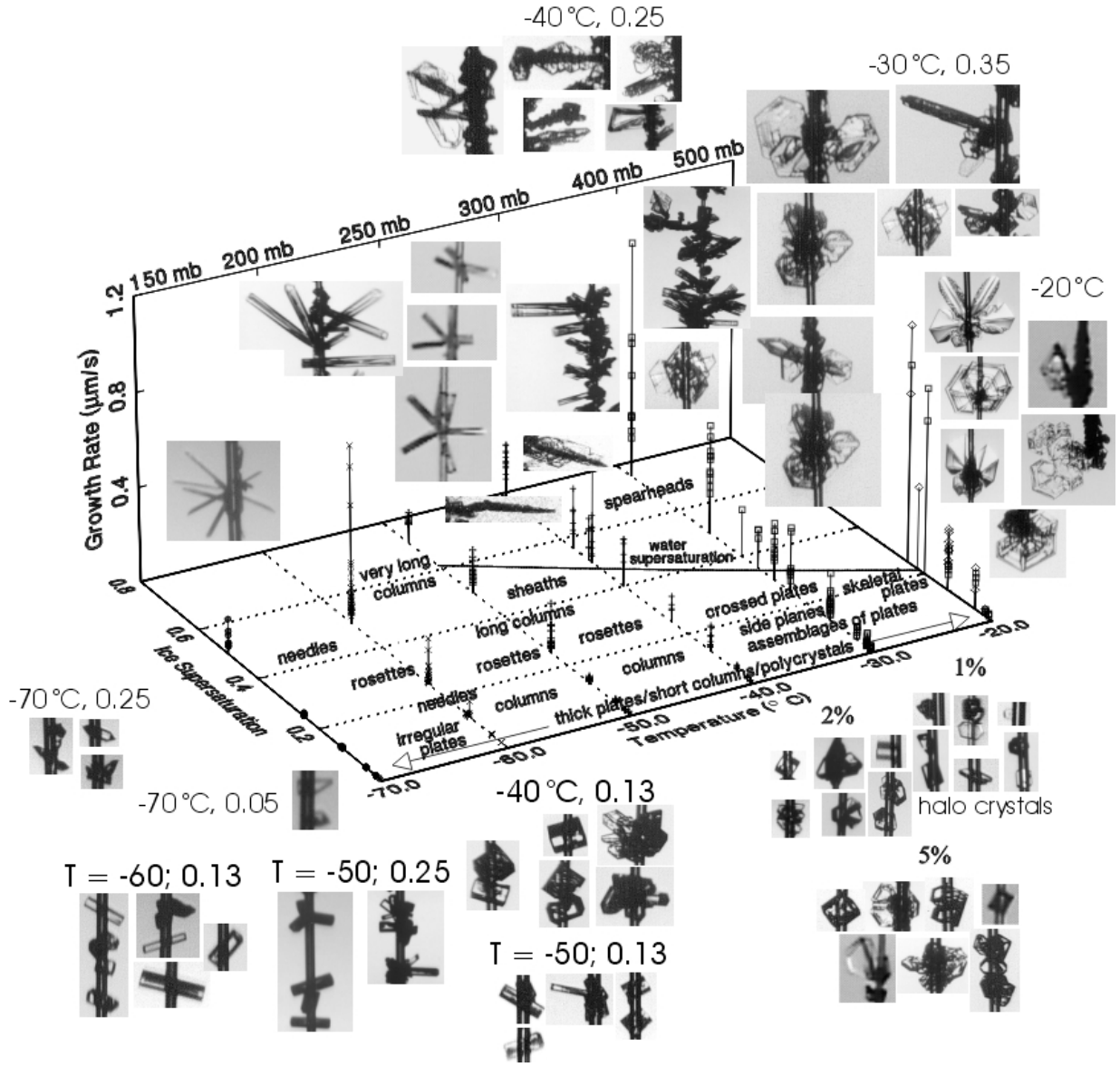

Figure 3. A sample of ice crystal habits for temperatures ranging from -20°C to -70°C, pressures ranging from 500 mb (hPa) to 150 mb, and ice supersaturations from 0.01 to 0.60. For scale, the crystals shown were grown on filaments with diameters of 50 : m to 70 : m. Crystal habits for ice supersaturations of 1%, 2% and 5% at lower right are from growth at -20°C to -40°C. The habits shown for 1% and 2% ice supersaturation are indicative of the low supersaturation habit down to approximately -60°C and are essentially independent of temperature. The solid line in the middle of the graph represents ice supersaturation equivalent to water saturation and is extrapolated to -50°C.

One essential feature of figure 3 was stated earlier, namely that crystals are generally plate-like above -40°C and columnar below this temperature. Simple pristine plates and columns appear with high frequency only at low ice supersaturation as indicated at the bottom of the graph.

At -20°C crystals appear as plates and skeletal plates at low to moderate supersaturation, skeletal plates often containing hopper patterns. Columns were rarely observed at this temperature and were nearly equiaxed when seen. At low supersaturation, polycrystals are nugget-like and irregularly faceted or plate-like with many raised layers of differing thicknesses. At higher supersaturations, polycrystals appear as crossed plates, frequently in a form best described as parallel crossed plates (pcp) which consists of assemblages of thin slightly overlapping plates growing from a common center which are not coplanar but have their c axes aligned in the same direction. An example of this type can be seen at the right of figure 3 consisting of several skeletal plates growing from the side of a an irregular polycrystal. Intersecting crossed plates (cp) as described by Furukawa and Kobayashi (1978)are occasionally observed. Near water saturation, large thin sector-like plates and dorites (Hallett et al. 2001) are observed which appear to be a continuation of forms observed at -15°C to -18°C but at supersaturations below those required for dendritic forms.

At -30°C, the low supersaturation habits are similar to those seen at -20°C except that short columns with length (L) to width (w) ratios of 1.4#L/w#2 are observed with low frequency. For higher supersaturations, the habits observed at -30°C are much more complex and variable than those at -20°C and consist of crossed plates (cp and pcp), radiating and irregular assemblages of plates, side plane types (sdpl), gohei twins, scrolls, and spearhead types, both bare (shb) and with side planes (sdpl). Kajikawa et al. (1980) described a number of subcategories of side plane types, and descriptions of these and others can be found in Kikuchi (1970), Kikuchi and Kajikawa (1979) and Sato and Kikuchi (1989). The transition to this more complex regime actually begins at approximately -25°C. One advantage of using a static diffusion chamber is that a spectrum of temperatures and supersaturations can be simultaneously observed (see figure 1) so that transitions between habit regimes are readily observable.

The habits at -40°C are very similar to those seen at -30°C with columns appearing with slightly higher frequency but still generally short with length to width ratios of 1.4#L/w#2.5. Intersecting crossed plates (cp) appear with highest frequency between -35°C and -40°C. A transition from predominantly plate-like to columnar behavior begins to occur at -38°C which is especially evident near water saturation as can be seen in the image in figure 3 just below the 500 mb symbol. A mixture of complex plate-like polycrystals and short sheaths begin to appear at this temperature with a fairly sharp transition to columnar forms just below -40°C.
Below -40°C and at supersaturations around 25% with respect to ice, bullet rosettes begin to appear and increase in frequency with increasing supersaturation. In this region, columns and bullets typically have length to width ratios of 2#L/w#5, aspect ratio increasing with increasing supersaturation and decreasing temperature. Bullet rosettes typically have 2 to 6 bullets with 3 being the most common.

The habits at -50°C are essentially a continuation of those seen just below -40°C except that the aspect ratios of columns and bullets are generally larger than those seen at higher temperatures. Crossed plates and other plate-like polycrystals are observed below -40°C but with decreasing frequency such that they are rarely seen at -50°C.

At or below -50°C and at moderate ice supersaturation, the habit consists of long solid columns whose aspect ratios increase with increasing supersaturation leading to the appearance of long hollow sheaths at ice supersaturations in excess of 40%. Near -55°C at moderate ice supersaturations, long thin needles begin to appear, increasing in frequency with decreasing temperature. Long column and needle rosettes begin to appear at ice supersaturations in excess of approximately 25%, needles and needle rosettes becoming more frequent with decreasing temperature.

At -70°C, needles and needle rosettes dominate the habit above an ice supersaturation of 25%, however, at lower supersaturation, odd looking sharply cornered crystals which appear transitional between plates and needles are often observed, some of which exhibit trigonal symmetry. Solid columns are also occasionally observed. Below -70°C, low supersaturation forms typically consist of

thin, faceted, irregular plates or compact irregular polycrystals.

6. HABIT FREQUENCIES AND GROWTH RATES

Habit frequencies have been calculated for the results presented in figure 3. Crystals have been categorized according to polycrystals, plates and columns as shown in figure 4 for crystals grown at -30°C. Polycrystalline forms are further divided into subcategories in figure 5.

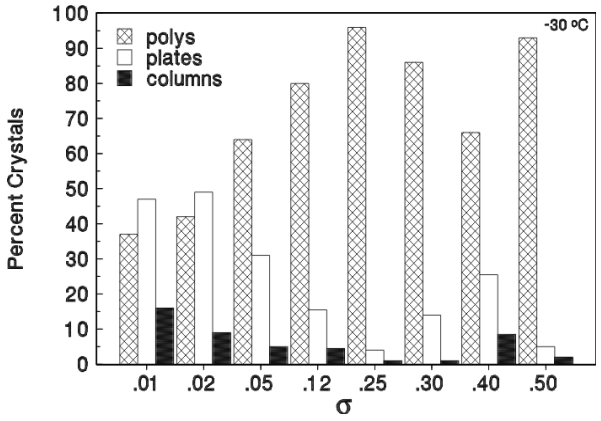

Figure 4. Habit distribution of crystals grown at -30°C.

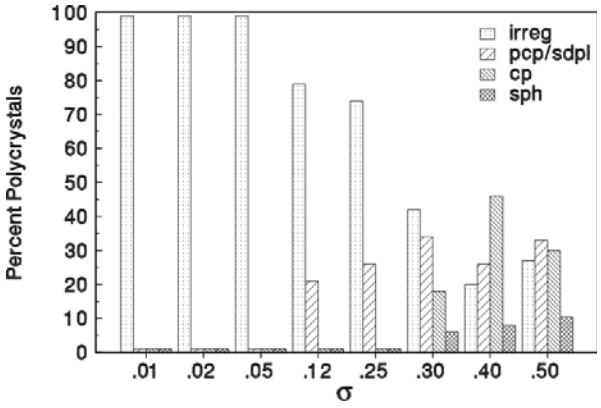

Figure 5. A breakdown of the polycrystalline forms in figure 4 grown at -30°C. Types indicated by pcp and cp are described above and sdpl stands for side plane types. "Irreg" represents irregular nugget and plate-like polycrystals at low supersaturation and irregular assemblages at higher supersaturations.

The measured maximum dimensional (D) growth rates (D = diameter = w for plate-like habits and D = L = length for columns) for these habit forms are shown in figure 6 along with habit specific linear fits of the growth data as a function of ice supersaturation.

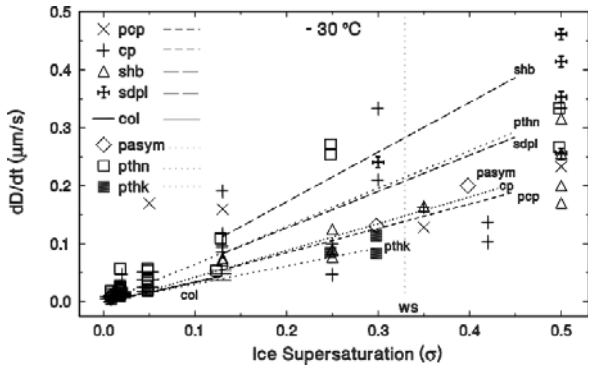

Figure 6. Maximum dimension growth rates for habits shown in figures 4 and 5. Habit specific linear fits of growth rates as a function of ice supersaturation are shown. Plates are described as thick (pthk), thin (pthn), and asymmetric (pasym). Polycrystalline forms are discussed in section 5.

One feature of the results in figure 6 is the large spread in growth rates, even for crystals of the same habit growing at the same ice supersaturation. This reflects a basic nonuniformity of crystal size and aspect ratio for crystals growing under similar conditions as shown for plates in figure 7.

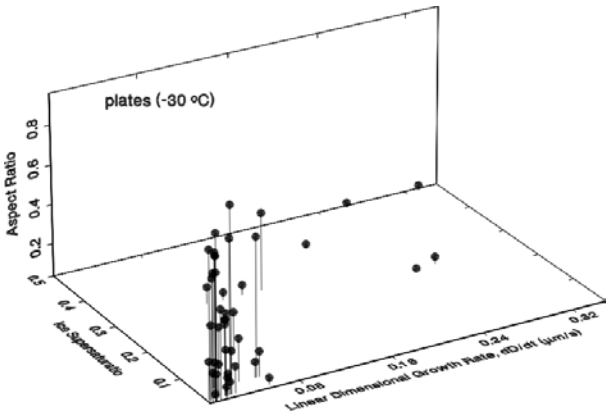

Figure 7. Maximum width growth rates and aspect ratios (h/w, h= height,w = width) for plates at -30°C.

Maximum projected area growth rates and volume growth rates are shown in figures 8 and 9.

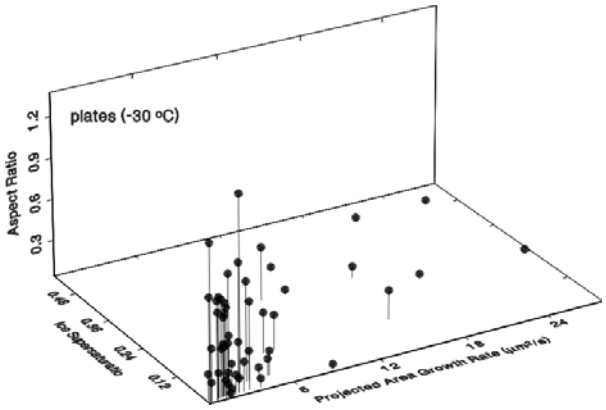

Figure 8. Projected area growth rates for plates as a function of aspect ratio (h/w, h = height, w = width) at -30°C.

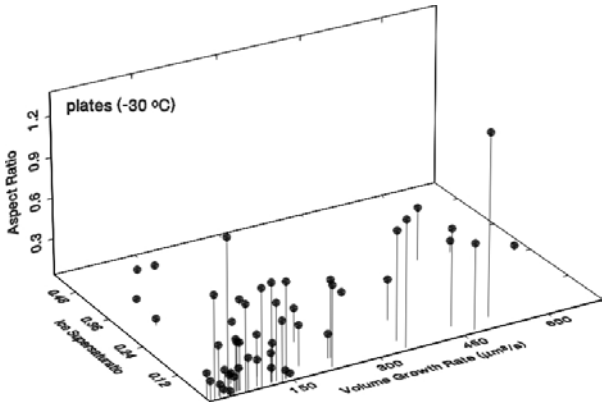

Figure 9. Volume growth rates for plates as a function of aspect ratio (h/w, h = height, w = width) at -30°C.

Similar plots for columns and polycrystals have been preformed at this and other temperatures and will be presented in a forthcoming paper. However, these figures indicate that crystal defects have a significant effect on crystal growth characteristic and are quite variable (Hallett et al. 2002). For instance, two crystals growing at the same temperature and supersaturation may have very different linear growth rates and thicknesses but similar volumes, or alternately may have similar linear growth rates but thicken at different rates resulting in very different volume growth rates.

With such variation of growth rates and habit, it may seem that calculating a representative growth rate is nearly impossible. However, by performing habit specific fits of growth rates and then weighting them by habit frequency, it appears that reasonable average growth rates can be obtained. This has been performed and is shown in figures 10, 11 and 12. Fitting growth rates as a function of ice supersaturation yields a slope which is an average growth rate normalized to ice supersaturation.

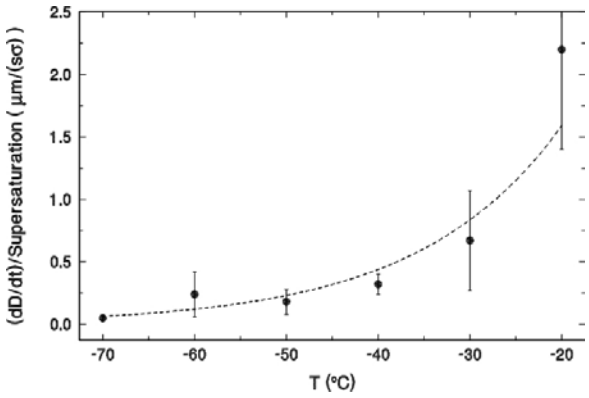

Figure 11. Average dimensional growth rates as a function of temperature and normalized according to ice supersaturation. To obtain a growth rate at a particular temperature and ice supersaturation, the normalized value is multiplied by the decimal supersaturation which yields the growth rate at that supersaturation and temperature.

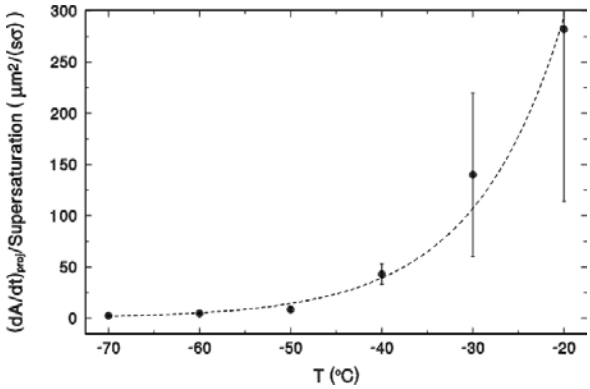

Figure 12. Average projected area growth rates normalized to ice supersaturation.

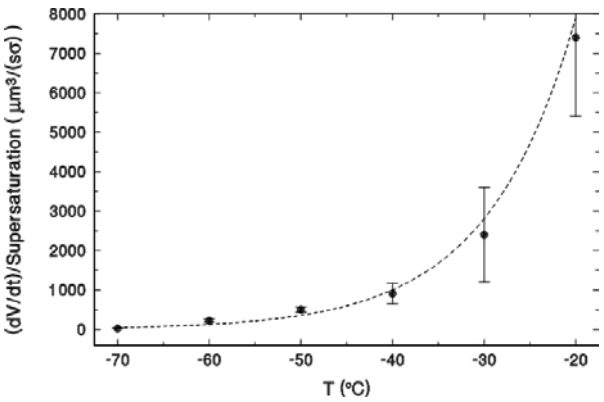

Figure 13. Average volume growth rates as a function of temperature and normalized according to ice supersaturation. To obtain a growth rate at a particular temperature and ice supersaturation, the normalized value is multiplied by the decimal supersaturation which yields the growth rate at that supersaturation and temperature.

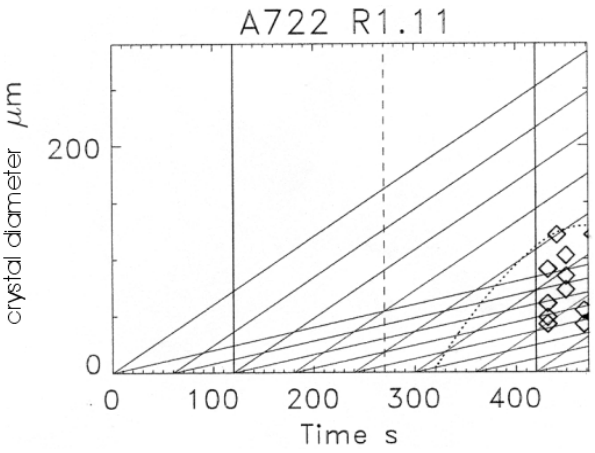

Figure 14. Estimated ice crystal growth trajectories. The area between the vertical solid lines is a region of water saturation. The vertical dashed line is the updraft-downdraft interface. The diamonds are ice crystal diameters obtained with the DRI cloudscope.

The error bars shown in these figures represent the variance in measured growth rates, the precision in measurement of any growth rate being considerably smaller.

A test case comparison of these results with in situ observations has recently been conducted by comparing predicted crystal dimensions with those observed by Field (2001, private communication) and Field et al. (2001) in an orographic wave cloud shown in figure 14. In that study, crystals were observed with the DRI Cloudscope after approximately 300 seconds of growth at a temperature of approximately -30 °C following the measurement of water saturation conditions with a Nevzorov probe. The particle observed ranged in size from 50 -125 : m as shown in figure 14. From the normalized growth rates shown in figure 11 at water saturation (an ice supersaturation of 0.33) and a temperature of approximately -30 °C, the data indicates a diameter growth rate of 0.33 x 0.7 or a growth rate of 0.23 : m/s. After 300 seconds this would yield an average crystal size of 70 : m, assuming at least some of the crystals nucleated when water saturation was reached as independently observed in this study (figure 2). From the variance, a spread of sizes of 25-120 : m is expected, an estimation which spans the observed crystal sizes.

A detailed presentation of habit results and growth rates at other temperatures is currently being submitted for publication and additional comparisons with in situ data will be performed. One of the most significant aspects of these comparisons is the predominant influence of polycrystalline habits which dominate the habit distributions at all temperatures presented in this study and at all ice supersaturations, except for very low values. This can be seen in the frequency plots of figures 15, 16 and 17.

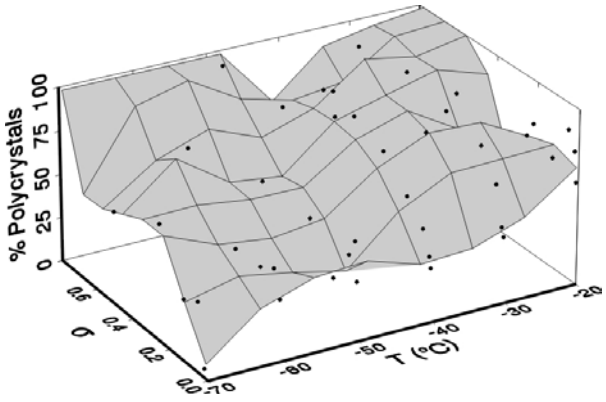

Figure 15. Frequency of polycrystalline ice habits as a function of temperature and ice supersaturation.

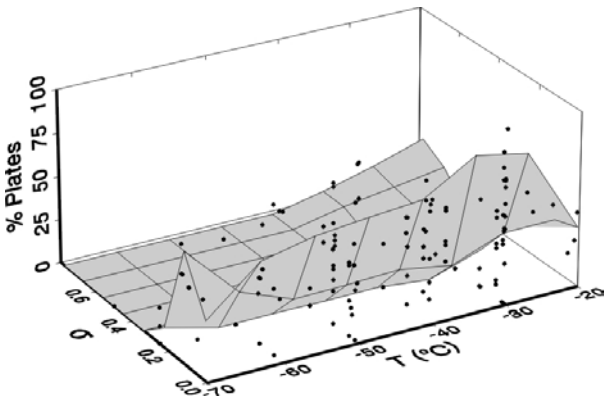

Figure 16. Frequency of plates as a function of temperature and ice supersaturation.

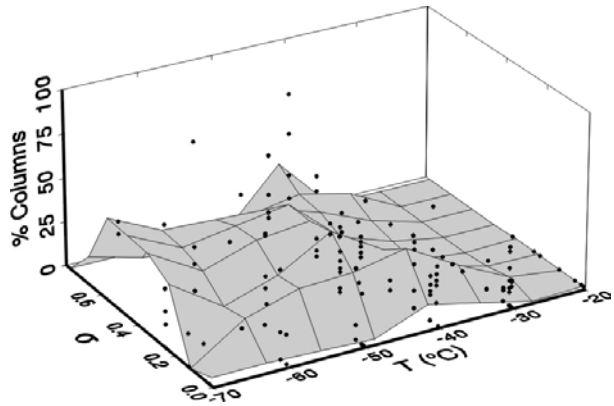

Figure 17. Frequency of columns as a function of temperature and ice supersaturation.

7. HALO PRODUCING HABITS

In the book "Atmospheric Halos", Tape (1994) notes that halo producing crystal populations in the antarctic are those dominated by simple plates and columns with smooth parallel facets. He also comments that while crystals with sizes of only 10 - 20 : m can produce faint halos, the strongest halos are produced by pristine crystals with sizes of 100-200 : m. However, Tape also notes that crystal populations of this size range are rarely pristine and are dominated by crystals with rough or irregular facets which do not produce halos. Tape observed that halo producing populations are rare in the antarctic and Hallett el al. (2002) discuss that they occur with even lower frequency elsewhere in the atmosphere. These observations together with the results from this study place strict limitations on the ice supersaturations capable of producing crystal populations which contain large numbers of pristine halo producing crystals.

A comparison of previous laboratory studies found in Bailey and Hallett (2002a) shows that the highest frequencies of pristine crystals is observed at very low ice supersaturation, typically no more than 2% as is the case in this study. Additionally, to achieve sizes of 100-200 : m, stable low supersaturation conditions must be maintained for time scales on the order of 30 to 90 minutes at -30°C and longer times at lower temperatures as in a shallow, long period, gravity wave. This is concluded from the growth rates of simple plates and columns shown in figure 18 where the normalized growth rates for pristine crystals are presented in comparison with the statistically averaged growth rates which represent the dominant polycrystalline forms at ice supersaturations above 5%.

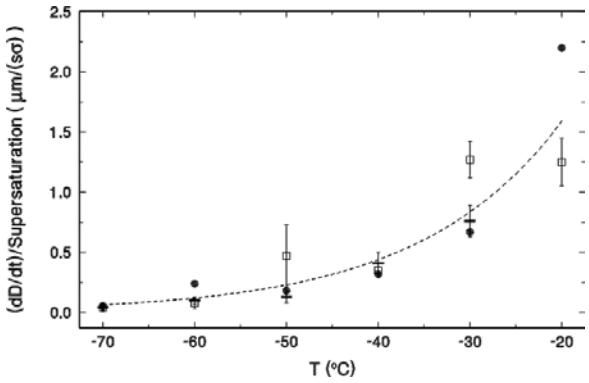

Figure 18. Comparison of pristine plate (squares) and column (horizontal bars) normalized growth rates at low ice supersaturation in comparison with with the results from figure 12. Data from ice supersaturations up to 2% are shown for -40°C # T# -20 °C, up to 5% at -50 °C, and up to 13% at -60 °C. Error bars represent variances due to aspect ratios.

The 5% growth images shown at lower right in figure 3 are from growth at temperatures from -20°C to -40°C and show that habits under these conditions are dominated by crystals which would not produce halos. Habit observations in this study

indicate that ice supersaturations up to 5% may produce pristine crystals with sufficient frequency to produce halos at temperatures below -40°C and possibly up to 13% at -60°C.

8. CONCLUSION

A new method for growing ice crystals in the laboratory which combines static diffusion and expansion techniques has produced a comprehensive set of crystal growth and habit data from -20°C to -70°C. Good correlation between in situ measurements and these laboratory results has been observed here and in Bailey and Hallett (2002a) where the critical aspects of nucleation in laboratory experiments have also been addressed. The results appear to provide a basis for improved cloud and radiation modeling and are being used as a guide for laboratory ice cloud growth and optical scattering experiments using a fall tower.

ACKNOWLEDGEMENTS

This research was supported by National Science Foundation, Physical Meteorology Program, Grant ATM-9900560 and National Aeronautics and Space Administration Grant NAG-1-2046. Laboratory cloud experiments are supported by the United States Air Force.

REFERENCES

Bailey, M. and J. Hallett 2000: Nucleation, growth and habit distribution of cirrus type crystals under controlled laboratory conditions. *13th International Conference on Clouds and Precipitation*, August 14-18, 2000, Reno, Nevada, pp. 629-632.

Bailey, M. and J. Hallett, 2002a: Nucleation effects on the habit of vapour grown ice crystals from -18 °C to -42 °C. *Quart. J.R. Met. Soc.* (accepted for publication).

Bailey, M. and J. Hallett 2002b: Growth rates and habits of ice crystals from -20°C to -70 °C (submitted for publication).

Field, Paul R., 2001 (private communication)

Field, Paul, R., R.J. Cotton, K.Noone, P. Glantz, P.H. Kaye, E Hirst, R.S. Greenway, C. Jost, R. Gabriel, T. Reiner, M. Andreae, C. P. R. Saunders, A. Archer, T. Choularton, M. Smith, B. Brooks, C. Hoell, B. Brandy, D. Johnson and A. Heymsfield, 2001: Ice nucleation in orographic wave clouds: Measurements made during INTACC. *Quart. J.R. Met. Soc.*, **127**, 1493-1512.

Furukawa, Y. and T. Kobayashi, 1978: On the growth mechanism of polycrystalline snow crystals with a specific grain boundary. *J. Crys. Gr.*, **45**, 57-65.

Hallett, J., W.P. Arnott, M.P. Bailey and J.T. Hallett, 2001: Ice crystals in cirrus. in *Cirrus*, Editors D.K. Lynch, K. Sassen, D.O. Starr, G. Stephens, Oxford University Press, 2002, Ch. 3, pp 41-77.

Kajikawa, M.., K. Kikuchi, and C. Magono, 1980: Frequency of occurrence of peculiar shapes of snow crystals. *J. Meteor. Soc. Japan*, **58**, 416-421.

Keller, V.W. and J. Hallett, 1982: Influence of air velocity on the habit of ice crystal growth from the vapor. *J. Cryst. Growth*, **60**, 91-106.

Kikuchi, K., 1970: Peculiar shapes of solid precipitation observed at Syowa Station, Antarctica. *J. Meteorol. Soc. Jpn.*, **48**, 243-249.

Kikuchi, K. and M. Kajikawa, 1979: Comments on v-shaped snow crystals observed in Arctic Canada *J. Meteor. Soc. Japan*, **57**, 484-487.

Sato, N. and K. Kikuchi, 1989: Crystal structure of typical snow crystals of low temperature types. *J. Meteorol. Soc. Jpn.*, **48**, 521-528.

Tape, W., *Atmospheric halos: Antarctic research series, 64*, American Geophysical Union, Washington, D.C., 1994.